Delivery report

PV-LAC: advances Land, Aerosol and Coastal products for Proba-V

PV-LAC: D-6-A2 Validation report Activity 3

Sindy Sterckx, Liesbeth De Keukelaere, Stefan Adriaensen, Els Knaeps

May 2017

DISTRIBUTION LIST

Author(s)	:	Sindy Sterckx, Liesbeth De Keukelaere, Stefan Adriaensen, Els Knaeps
Reviewer(s)	:	Philippe Goryl, Fabrizio Niro
Approver(s)	:	Philippe Goryl, Fabrizio Niro
Issuing authority	:	VITO

CHANGE RECORD

Release	Date	Pages	Description of change	Editor(s	Reviewer(s)
V1.1	3/05/2017	All	First version	Sindy Sterckx, Liesbeth De Keukelaere ,Stefan Adriaensen ,Els Knaeps	Philippe Goryl, Fabrizio Niro
V2	3/10/2017	all	All figures/results updated Comparisons with MODIS added	Sindy Sterckx, Liesbeth De Keukelaere	Philippe Goryl, Fabrizio Niro

TABLE OF CONTENTS

LIST OF FIGURES

LIST OF TABLES

ACONYMS

A/C	Atmospheric Correction
ACIX	Atmospheric correction intercomparison exercise
AERONET-OC	Aerosol Robotic Network – Ocean Colour
AOT	Aerosol Optical Thickness
ASCII	American Standard Code for Information Exchange
ATBD	Algorithm Theoretical Basis Document
CEOS	Committee on Earth Observation Satellites
DISORT	DIScrete Ordinate Radiance Transfer
ECMWF	European Centre for Medium-Range Weather Forecast
FTU	Formazin Turbidity Unit
iCOR	Image CORrection for land and water
IODD	Input-output Definition Document
LUT	Look-Up Table
MODIS	Moderate Resolution Imaging Spectroradiometer
MODTRAN	MODerate resolution atmospheric TRANsmission
NDVI	Normalized Difference Vegetation Index
NIR	Near-Infrared
NTU	Nephelometric Turbidity Unit
OPERA	Operational atmospheric correction for Land and Water
RAA	Relative azimuth angle
S1	1-daily synthesis
SM	Status map
SMAC	Simplified Method for Atmospheric Correction
SNR	Signal-to-Noise Ratio
SWIR	Shortwave Infrared
SZA	Solar zenith angle
TOA	Top-of-Atmosphere
TOC	Top-of-Canopy
TSM	Total Suspended Matter
VITO	Vlaamse Instelling voor Technologisch Onderzoek
VZA	Viewing zenith angle

CHAPTER 1 INTRODUCTION

This is the second version (V2) of the Validation Report for the PV-LAC coastal activities.

The structure of the document is as follow:

CHAPTER 2 provides the validation results of the atmospheric correction applied to the primary validation site. Both the intermediate AOT products and the water leaving reflectance values are compared against in-situ measurements performed at coastal AERONET (OC) stations. For the atmospheric correction two approaches are inter-compared: (1) spatial extension of the AOT values retrieved from nearby land and (2) retrieval of aerosol information from the SWIR band following a SWIR black pixel approach over water.

CHAPTER 3 gives the validation results of the single-band turbidity retrieval algorithm applied to PROBA-V data from the primary validation site. PROBA-V retrieved Turbidity values are compared against turbidity data from fixed buoys and a comparison is made against MODIS turbidity maps.

In CHAPTER 4 the validation results of the A/C methods applied to PROBA-V data from the global test sites are given. AERONET OC sites included in the report are Venice, LISCO and MVCO.

CHAPTER 2 A/C VALIDATION ON PRIMARY VALIDATION SITE

2.1. INTRODUCTION

In this chapter we present and discuss the validation results of the atmospheric correction applied to PROBA-V data from the primary validation site, i.e. the Belgian coastal waters.

As discussed in the ATBD, two A/C methods are considered:

1) A/C based on spatial extension of aerosol information retrieved from nearby land (hereafter referred to as "iCOR land-based")
2) A/C based on extending the "black pixel" approach to the SWIR. The SWIR black pixel approach assumes that the contribution of in-water constituents is zero due to the high absorption of pure water in the SWIR. The signal in the SWIR can thus be assumed to be entirely atmospheric and can therefore be employed for the aerosol determination. land (hereafter referred to as "iCOR SWIR-based")

The validation is performed on 100 m PROBA-V data, acquired between 15 May 2014 and 31 December 31 2016 from the area given in Figure 1.

Figure 1: Study area of primary validation site.

The area is significantly larger than the originally foreseen Belgian coastal water site. An extension of the area was done because of several reasons: 1) through the extension more coastal AERONET stations can be used for the AOT validation, 2) for the validation of the turbidity results fixed buoys mainly located in UK waters are used, and 3) through the inclusion of clear and /or offshore waters

we can have a better understanding of the performance of the selected A/C approach and/or PROBA-V SNR issues in cleared offshore waters.

In the sections below we present the validation results from both the land-based and the SWIR based iCOR A/C where we focus first on the direct validation of the retrieved aerosol optical thickness (AOT) and next on the direct validation of the water-leaving reflectance values.

2.2. AOT VALIDATION

2.2.1. APPROACH

For evaluating the performance of the AOT retrieval approaches the retrieved AOT (550 nm) values are compared against the AOT (550 nm) Level 1.5 (Real Time cloud-screened) values measured by AERONET CIMEL instruments located at coastal sites within the study area. In Figure 2 the location of the AERONET stations are given.

As the iCOR SWIR-based approach only provides AOT results over water pixels, only AERONET–Ocean Color (AERONET-OC) sites can be used for validation of the SWIR-based AOT retrieval. The nearshore MOW1 platform (51.36°N; 3.12°E) located 5 km from the harbor of Zeebrugge and the offshore Thornton_C-power platform site (51.53°N; 02.96°E) located at 26 km from the coast are used in the study. It should be noted that some of the AERONET stations were not active for the whole 2014-2016 period.

The threshold for the temporal offset between the time of the PROBA-V overpass and AERONET measurement was set to ± 30 minutes.

Figure 2: Location of the AERONET stations used for AOT validation .

2.2.2. RESULTS

Figure 3 gives the scatter plots of AERONET AOT versus PROBA-V retrieved AOT (550nm) values for respectively the land-based and the SWIR based atmospheric correction (A/C) approach. The SWIR-based method only contains results for AERONET stations situated in water. iCOR land-based has results for both: land and water AERONET stations.The SWIR-based approach seems to systematically overestimate the AERONET-OC AOT values, with an offset of 0.15, while the land-based approach overestimates the AOT at low AOT-values, but underestimates at higher AOT values (>~0.2, regression slope lower than 0.5) for the AERONET-OC stations. Overall, the SWIR-based approach with a R^2 of 0.46 performs better than the land-based approach with a R^2 of 0.22 for the AERONET-OC stations. However, the land AERONET stations the land-AOT approach gives better results. This suggests that the lower correlation at AERONET-OC stations for land-AOT is due to the spatial extrapolation.

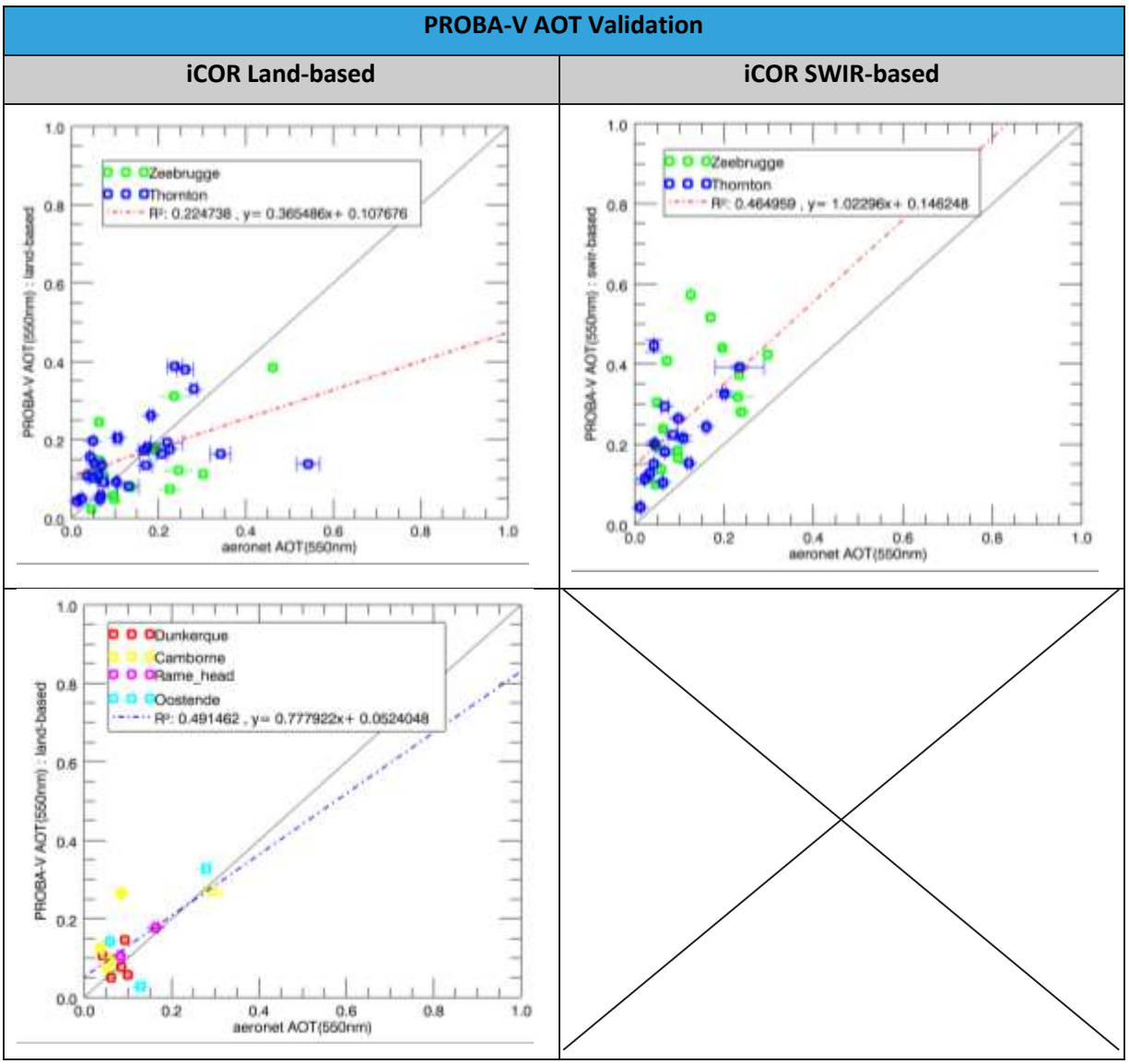

Figure 3: Scatter plots of AERONET AOT versus PROBA-V retrieved AOT (550 nm) values for respectively the land-based and the SWIR based A/C approach. The solid black line is the 1:1 line, dotted RED line is the regression line. The Y-error bar gives the standard deviation of PROBA-V

derived AOT values within a 1km x1km box around the AERONET location. The X-error bar gives the standard deviation of the AERONET AOT within max 30 min of PROBA-V acquisition.

2.3. RWN VALIDATION

2.3.1. APPROACH

The retrieved PROBA-V water leaving reflectance values are compared with the corresponding in-situ AERONET-OC measurements from the MOW1 platform and the Thornton_C-power platform. For this the normalized water leaving radiances ($L_{wn} = \rho_w . F_0/\pi$), measured by AERONET-OC CIMEL instruments are converted to water leaving radiance reflectance (ρ_w).

As can be seen in Figure 4, the PROBA-V spectral bands are much broader than the AERONET-OC spectral bands, which complicates the "direct" comparison. In order to take into account the difference in center wavelength and band width "a spectral shift" correction is applied before performing the "direct" comparison.

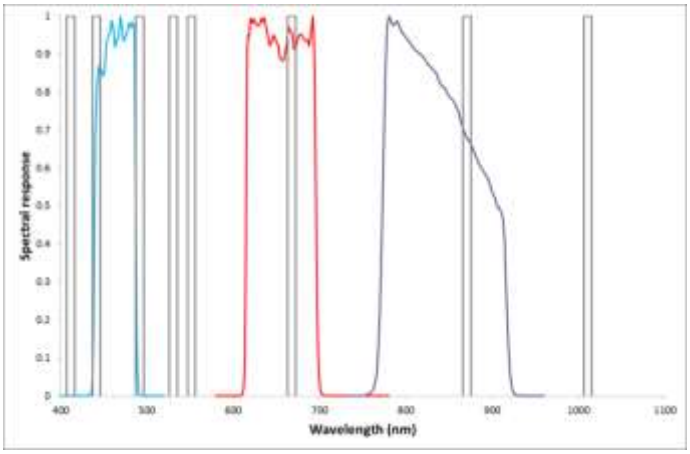

Figure 4: Comparison of spectral response of AERONET-OC (in grey) and PROBA-V spectral bands.

To determine the spectral shift correction coefficients, hyperspectral in-situ measured ρ_w spectra acquired from the North Sea from the Coastcolour dataset are used. In Figure 5, the spectral shift correction functions for the blue and red band based on Coastcolour dataset from the North Sea are given. For more details on the spectral shift correction we refer to the ATBD.

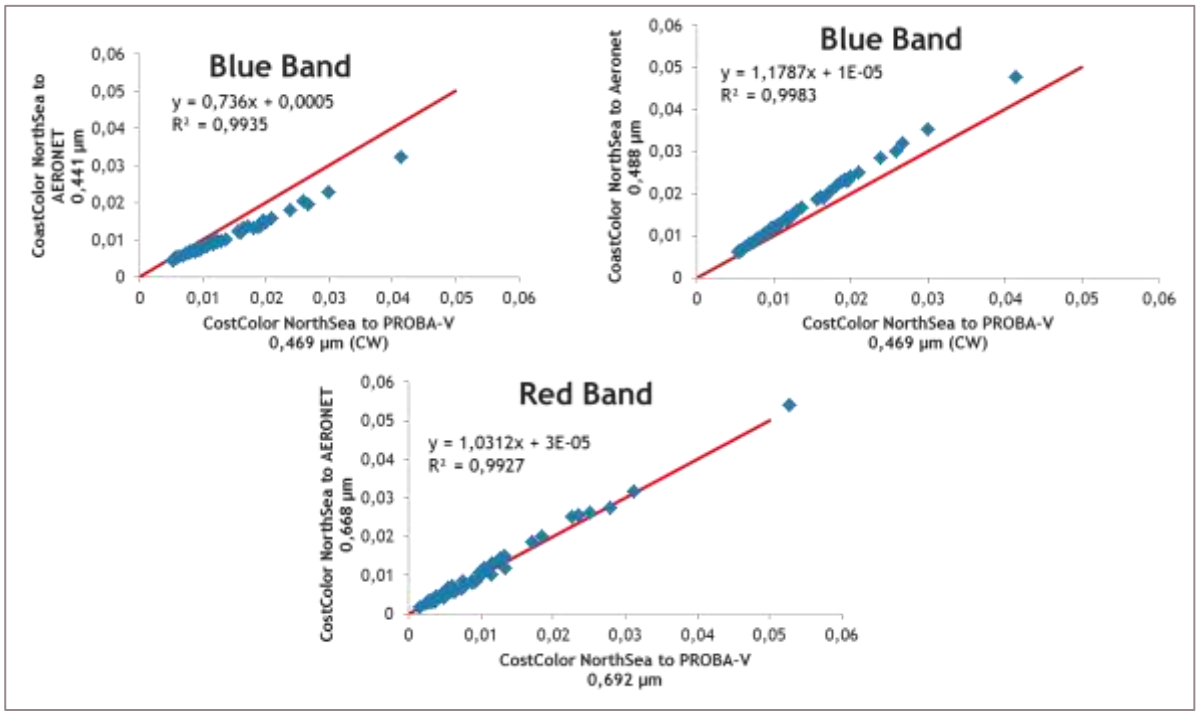

Figure 5. Spectral shift correction functions for the blue and red band based on Coastcolour dataset from the North Sea.

2.3.2. RESULTS

Figure 6 shows the validation results from the Thornton and Zeebrugge AERONET-OC stations for the PROBA-V water leaving reflectance in the blue, red and NIR band. The PROBA-V reflectances are converted using the coefficients from Figure 5.

For all the VNIR bands both the SWIR based approach outperforms the land-based approach. For the SWIR based approach a strong correlation is found with the in-situ measured water reflectance in the blue and red band with a R^2 of respectively 0.78 and 0.85. The land-based approach tends to systematically overestimate the water leaving reflectance values. This might be related to the underestimation of the AOT as shown in section 2.2.2.

For the NIR band the correlation between the AERONET-OC water reflectance and the PROBA-V water reflectance is very low probably due to the low SNR for the very low NIR radiances. This suggests that the PROBA-V NIR band cannot be used to derive turbidity in low to moderately turbid waters.

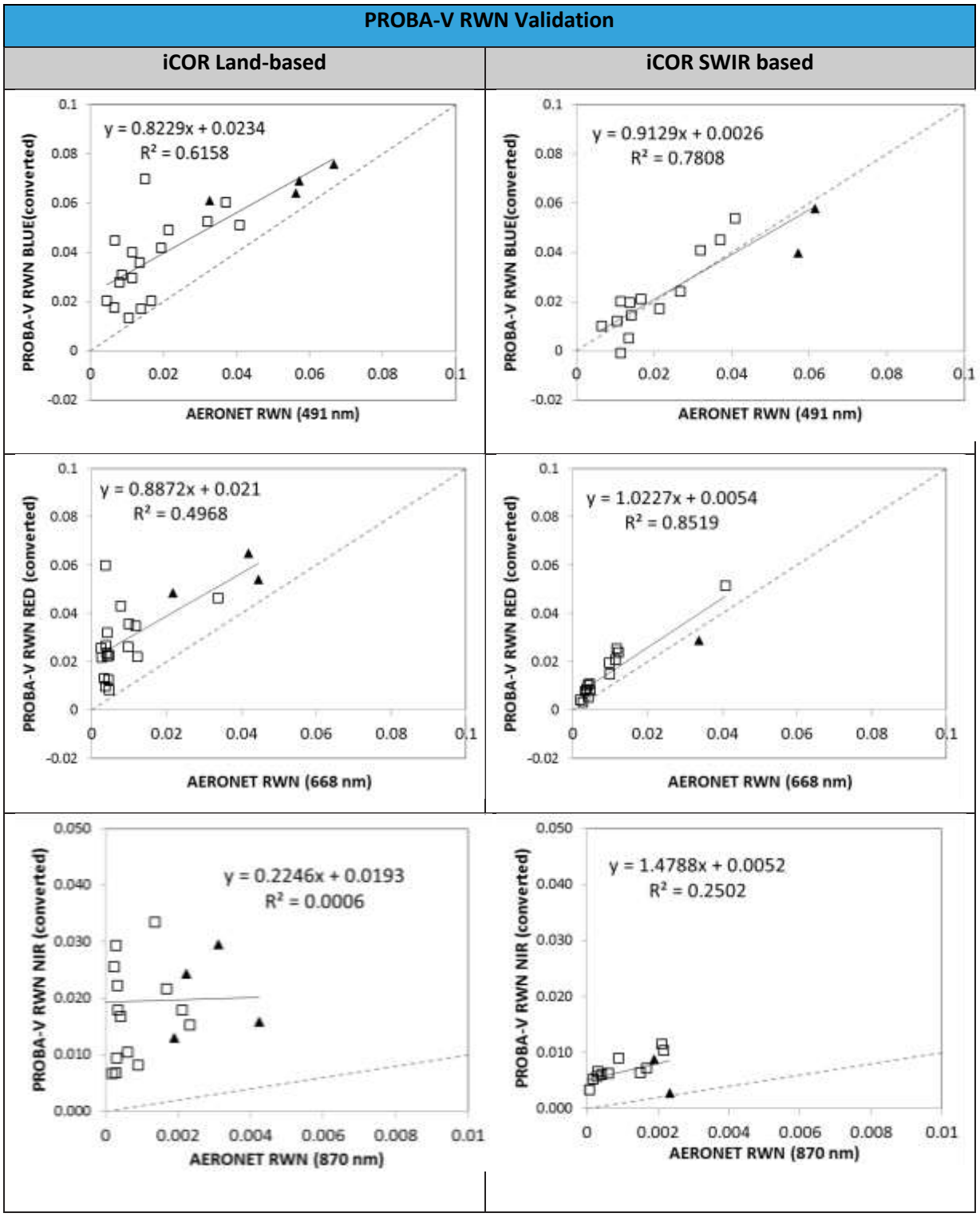

Figure 6: Regression plots of the water leaving reflectance from in situ (AERONET-OC) and from PROBA-V. The squares are results from the Thornton AERONET-OC station, the triangles are results from the Zeebrugge-MOW AERONET-OC station.

CHAPTER 3 PROBA-V TURBIDITY VALIDATION ON PRIMARY VALIDATION SITE

3.1. INTRODUCTION

The one-band algorithm developed by Nechad et al. (2009) is selected to derive turbidity from the PROBA-V water reflectance. The algorithm relates turbidity (T, in FNU) to the water reflectance ρ_w through,

$$T = \frac{A_T^{\rho} \cdot \rho_w(\lambda)}{\left(1 - \frac{\rho_w(\lambda)}{C_T^{\rho}}\right)} \quad (1)$$

where A_T^{ρ} and C_T^{ρ} are wavelength dependent calibration coefficients. In the linear region where $\rho_w(\lambda) << C_T^{\rho}$ the C_T^{ρ} has a very minor impact on the retrieved turbidity. Therefore an error in C_T^{ρ} will have a negligible impact in the linear region. C_T^{ρ} is calculated using standard inherent optical properties. The A_T^{ρ} coefficient was obtained by a non-linear regression analysis using in situ measurements of T an ρ_w and tabulated for every 2.5 nm in Nechad et al. (2009) and later improved in Dogliotti et al. (2011) (only for MODIS bands) based on an extended set of in-situ data. In Table 1 the C_T^{ρ} and A_T^{ρ} for the PROBA-V RED and NIR bands are given. For the calculation of A_T^{ρ} (NIR) the tabulated values in Nechad et al. (2009) are spectrally resampled and the retrieved value is adjusted considering the percentage change proposed by Dogliotti et al (2011) with respect to the Nechad et al. (2009) values.

Table 1: Resampled calibration coefficients $\boldsymbol{A_T^{\rho}}$ and $\boldsymbol{C_T^{\rho}}$ used to retrieve T for the PROBA-V RED and NIR bands.

PROBA-V band	$\boldsymbol{A_T^{\rho}}$(resampled)	$\boldsymbol{C_T^{\rho}}$(resampled)
RED $(583 - 732\ \mathrm{nm})$	237.891	0.168
NIR $(743 - 942\ \mathrm{nm})$	2535.41	0.209

The turbidity algorithm given in equation 1 is applied to the PROBA-V RED-band water leaving reflectance images generated on the basis of both the land-based and the SWIR based approach.

3.2. VALIDATION APPROACH

The retrieved PROBA-V turbidity is validated using the CEFAS SmartBuoys (Figure 7,Table 2) (Mills et al, 2003). These autonomous systems are moored, automated, multi-parameter recording platforms used to collect marine environmental data. Turbidity data are typically collected every 30 minutes at 1m water depth. The data are freely available for research purposes.

In the North Sea study area there are three Buoys currently in operation. These are: 1) Warp (TH1) NMMP in the turbid waters of the Thames; 2) West Gabbard (mid 2016 replaced by West Gabbard2) and 3) Dowsing located more offshore. One more buoy outside the study area is used: the Liverpool Bay Coastal Observatory.

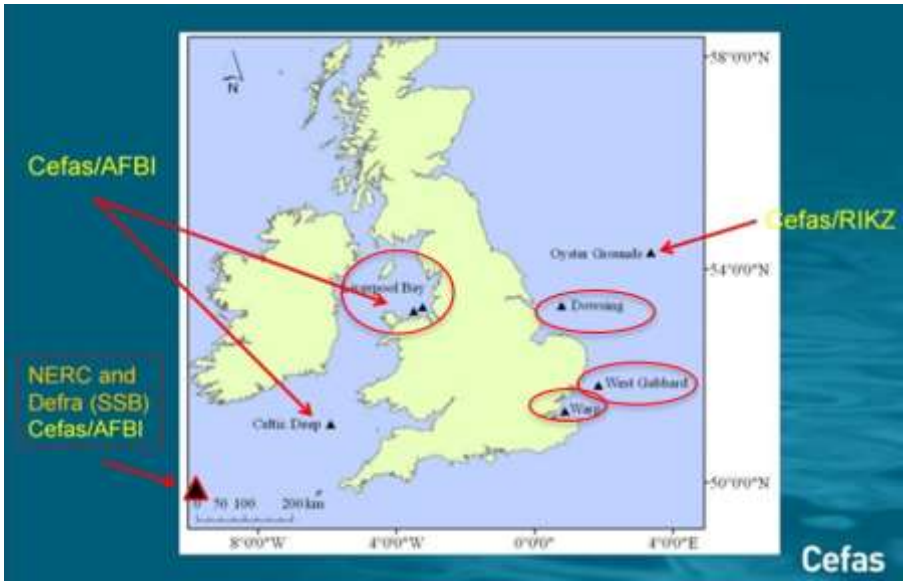

Figure 7: Location of Smartbuoys used for turbidity validation (marked with red circles).

Table 2: Coordinates Smartbuoy stations used for validation

Station name	coordinates
Warp (TH1) NMMP	51.52633°N 1.028167°E
Dowsing	53.53133° N 1.056°E
Liverpool Bay	53.5345°N 3.361833°W
West Gabbard *	51.98033°N 2.082833°E
West Gabbard2	51.9545°N 2.1097°E

*replaced by West Gabbard2 since May 2016.

For each PROBA-V overpass (over the test site) the turbidity of a nominal pixel containing the location of the field data measurement was extracted. The threshold for the temporal offset between the time of the PROBA-V overpass and field data measurement was set as ±1 hour.

Only valid observation were considered. Observations with a failure of the A/C, with high sun glint probability, or with a cloud percentage larger than 10% in the 1km x 1km region around the in-situ location were discarded in the results.

3.3. RESULTS

The validation results using the turbidity from the CEFAS smartbuoys are shown in Figure 8. A correlation with a R^2 of 0.73 between the PROBA-V derived turbidity values and the in-situ turbidity values is found when using the iCOR SWIR-based approach. The land-based A/C shows in general a positive bias which is probably caused by the atmospheric correction (offset already observed in the AOT and Rwn validation, see chapter 2).

Scatterplots have been made for all SmartBuoy location separately to see if the performance differs depending on the location (and turbidity level). No significant or clear dependency of the performance with the location could be found for the turbidity results obtained from PROBA-V

data corrected with the SWIR based approach. Even for the less turbid Dowsing site with Turbidity levels less than 6 FNU a relatively good correlation was found with the PROBA-V derived Turbidity values on the basis of the SWIR based A/C approach.

PROBA-V Turbidity validation	
iCOR Land-based	**iCOR SWIR based**
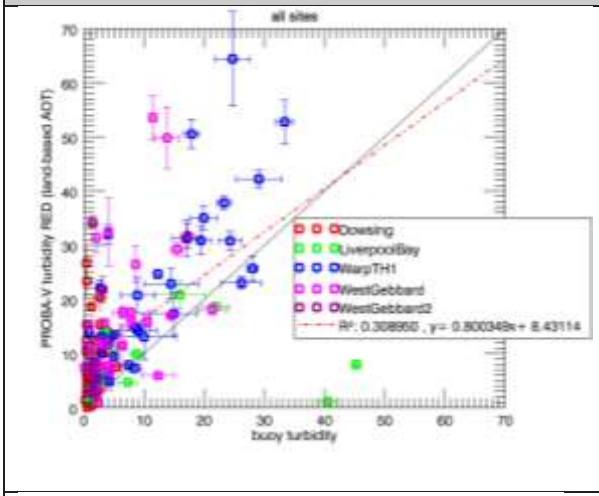	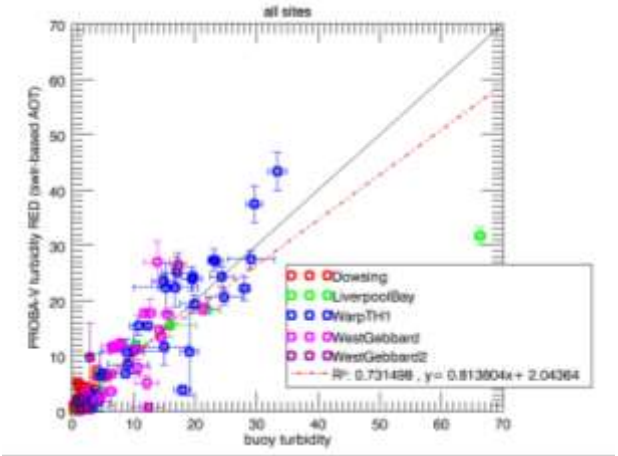
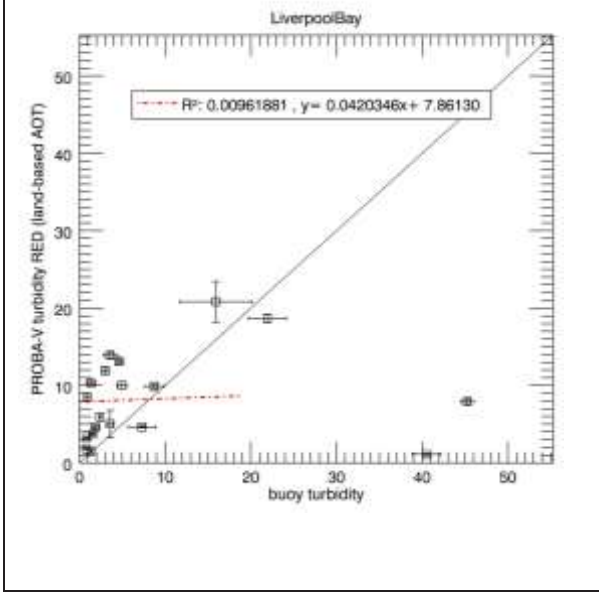	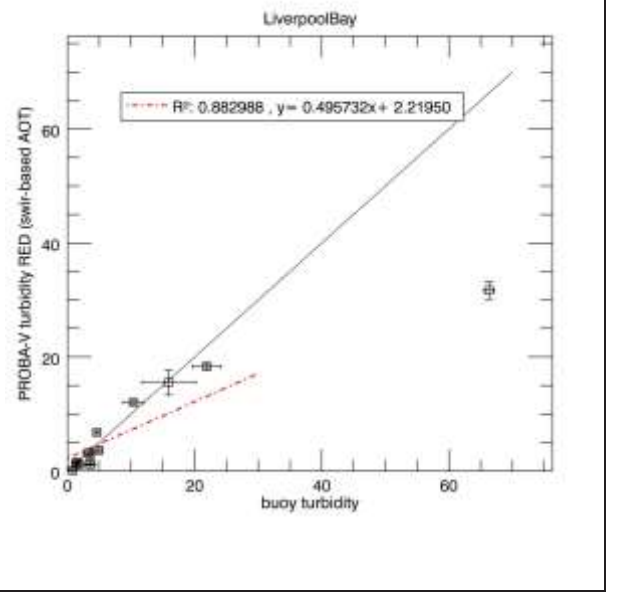

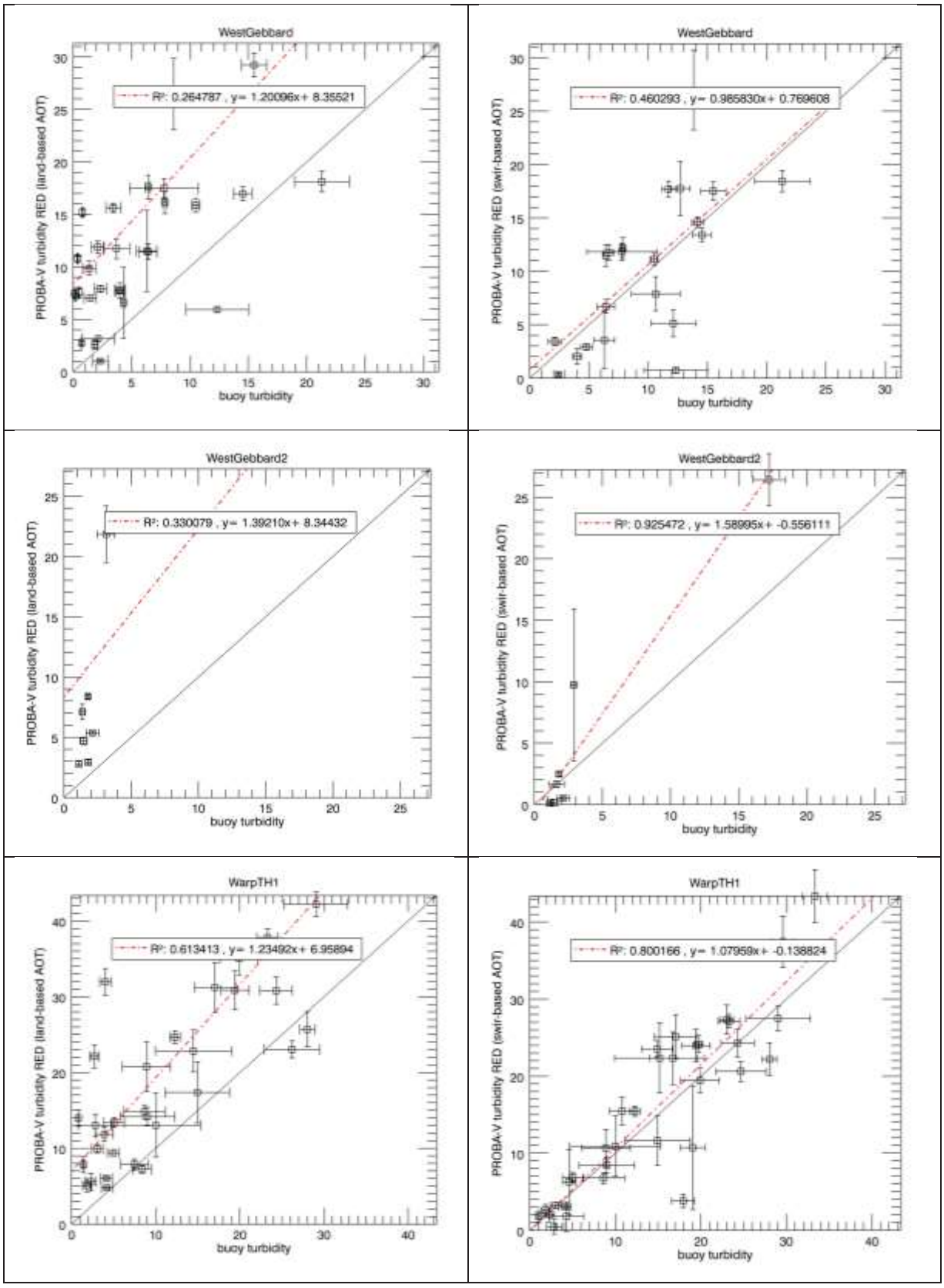
WestGebbard
R²: 0.264787 , y= 1.20096x + 8.35521
PROBA-V turbidity RED (land-based AOT)
buoy turbidity
WestGebbard
R²: 0.460293 , y= 0.985830x + 0.769608
PROBA-V turbidity RED (swir-based AOT)
buoy turbidity
WestGebbard2
R²: 0.330079 , y= 1.39210x + 8.34432
PROBA-V turbidity RED (land-based AOT)
buoy turbidity
WestGebbard2
R²: 0.925472 , y= 1.58995x + -0.556111
PROBA-V turbidity RED (swir-based AOT)
buoy turbidity
WarpTH1
R²: 0.613413 , y= 1.23492x + 6.95894
PROBA-V turbidity RED (land-based AOT)
buoy turbidity
WarpTH1
R²: 0.800166 , y= 1.07959x + -0.138824
PROBA-V turbidity RED (swir-based AOT)
buoy turbidity

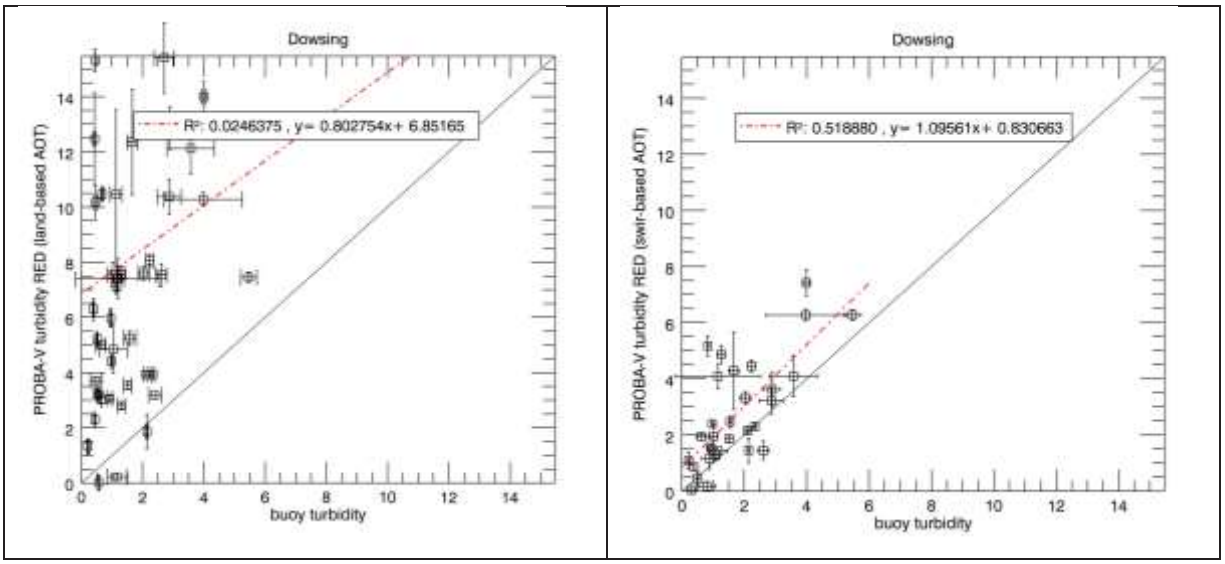

Figure 8: Regression plots between in situ and Proba-V turbidity for all the Smartbuoy locations. The Y-error bar gives the standard deviation of PROBA-V derived turbidity within the 1km x1km around the Smartbuoy location. The X-error bar gives the standard deviation of the buoy turbidity measurements performed within max. 1 hour of the PROBA-V acquisitions. The solid black line is the 1:1 line, dotted RED line is the regression line.

3.4. COMPARISON AGAINST MODIS TURBIDITY MAPS

Table 3 lists the MODIS Aqua and PROBA-V images used for the turbidity comparison validation. For each of these days a quicklook of the North Sea region for MODIS and PROBA-V are shown. MODIS data is processed with the HIGHROC S3plus processing chain, which makes use of the SeaDAS l2gen processor, following the Gordon & Wang aerosol approach (Gordan and Wang, 1994). For PROBA-V the two aforementioned A/C are considered: iCOR land-based and iCOR SWIR based. The turbidity maps were generated using the Dogliotti et al. (2011) algorithm for the red band on MODIS, and Nechad et al. (2009) adapted for the red band of PROBA-V as described in the ATBD. In first instance, a relative validation is performed between the MODIS and PROBA-V satellite products by comparing the patterns of turbidity. Invalid values in the turbidity products are coloured in white and can be linked to: (i) no data, (ii) clouds, (iii) negative values or (iv) AOT failure. Next to a relative validation, the absolute values are compared through boxplots.

When comparing the different turbidity maps visually (Figures 9 - 12), the MODIS and iCOR-SWIR based results are much alike, with the main difference that the higher resolution of PROBA-V becomes visible in the level of detail of sediment plumes in and around the Scheldt river. The iCOR-land based results show higher turbidity concentrations, which is in line with earlier observations in section 3.3. In the SWIR-based results, more pixels are flagged compared to iCOR land-based due to negative values. The extent of the boxplots for the four different days reveal as well that the range (without outlier) of PROBA-V land is larger and the median is higher than for MODIS.

Table 3: List of selected MODIS Aqua and PROBA-V images used for the intercomparison excercise.

Date	MODIS Aqua overpass	PROBA-V overpass	Time differece
03/04/2016	13:00	11:19	1:41
12/04/2016	12:55	11:20	1:35
01/05/2016	11:45	11:00	0:45
05/05/2016	13:00	11:11	1:49

Day 1 – 03/04/2016

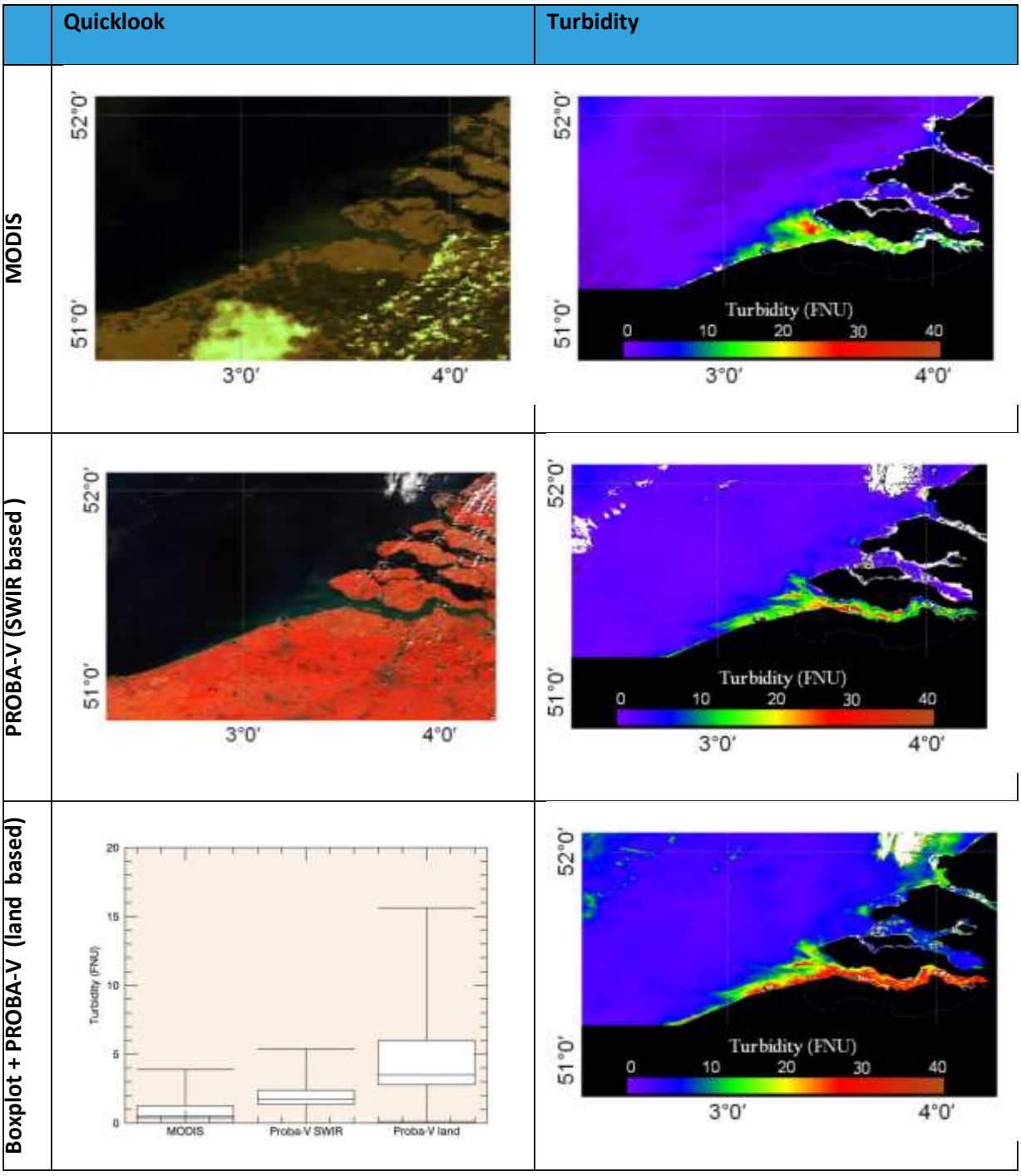

Figure 9: Quicklooks and turbidity maps generated for MODIS and PROBA-V, acquired on 03/04/2016. The latter using the iCOR-SWIR based and iCOR-land based method. The boxplots for the different results are plotted without outliers. Boxes represent the range between the 25th and 75th percentile, while the whiskers represent the 5th and 95th percentile.

Day 2 – 12/04/2016

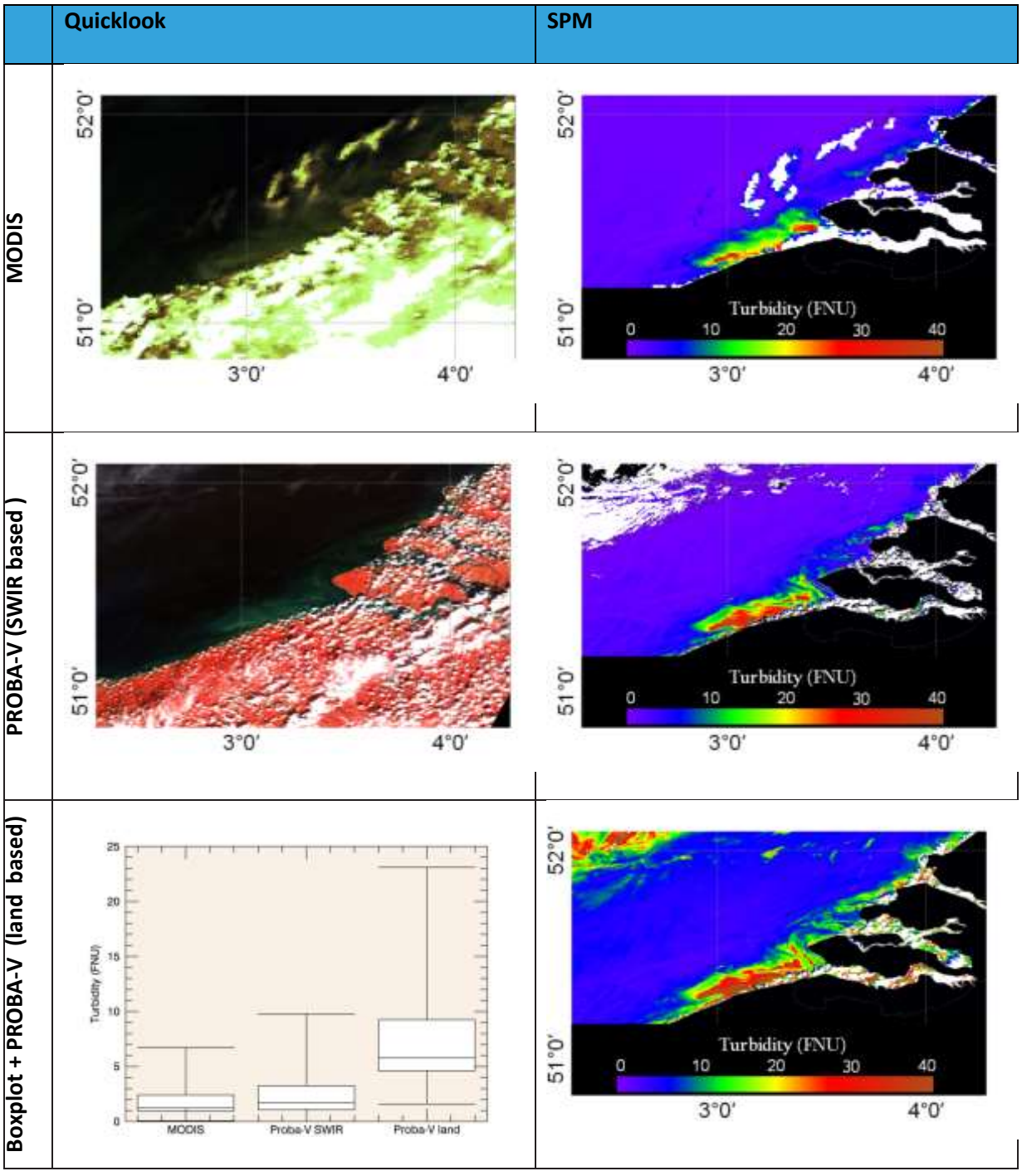

Figure 10: Quicklooks and turbidity maps generated for MODIS and PROBA-V, acquired on 03/04/2016. The latter using the iCOR-SWIR based and iCOR-land based method. The boxplots for the different results are plotted without outliers. Boxes represent the range between the 25th and 75th percentile, while the whiskers represent the 5th and 95th percentile.

Day 3 – 01/05/2016

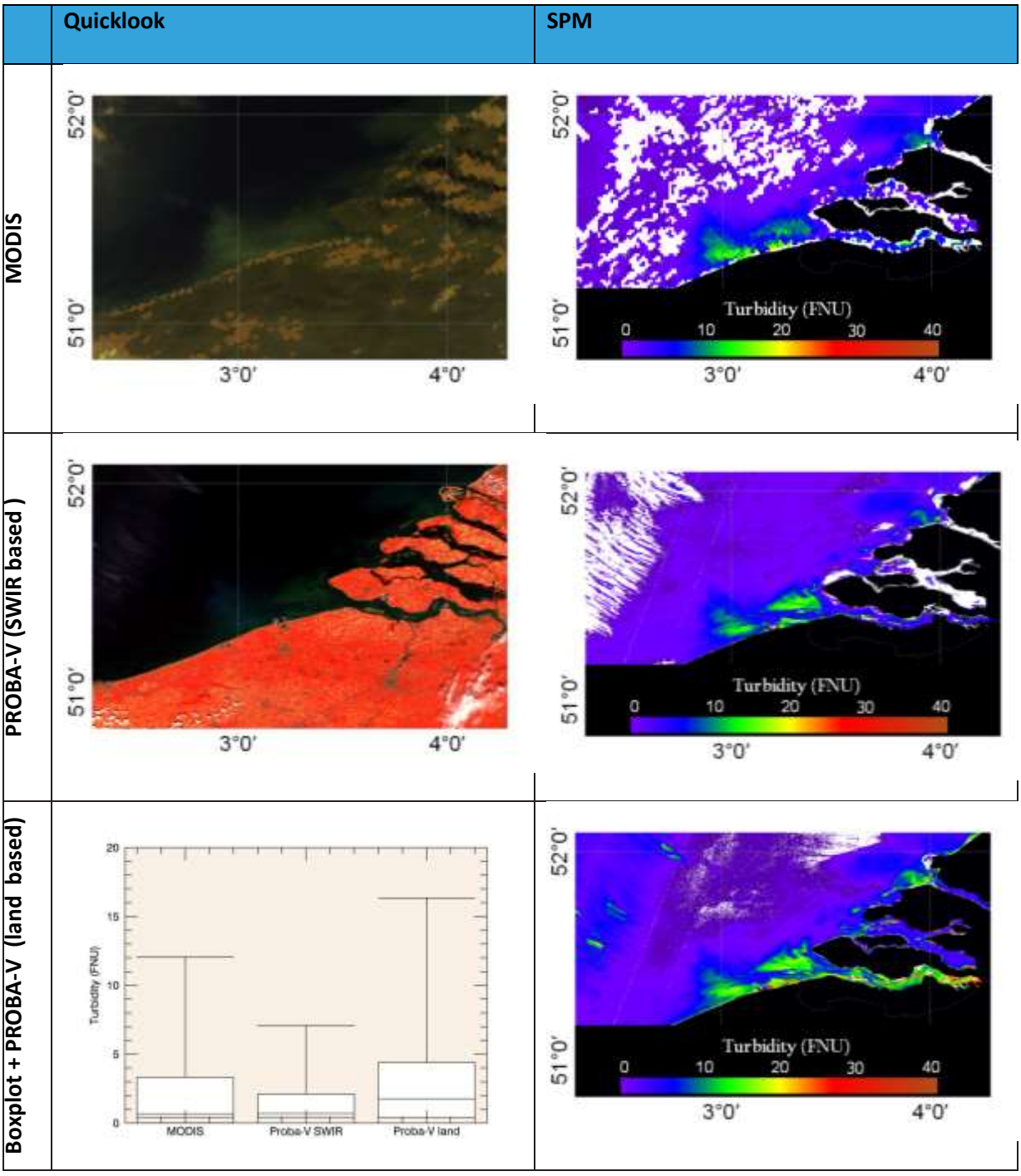

Figure 11: Quicklooks and turbidity maps generated for MODIS and PROBA-V, acquired on 03/04/2016. The latter using the iCOR-SWIR based and iCOR-land based method. The boxplots for the different results are plotted without outliers. Boxes represent the range between the 25th and 75th percentrile, while the whiskers represent the 5th and 95th percentile.

Day 4 – 05/05/2016

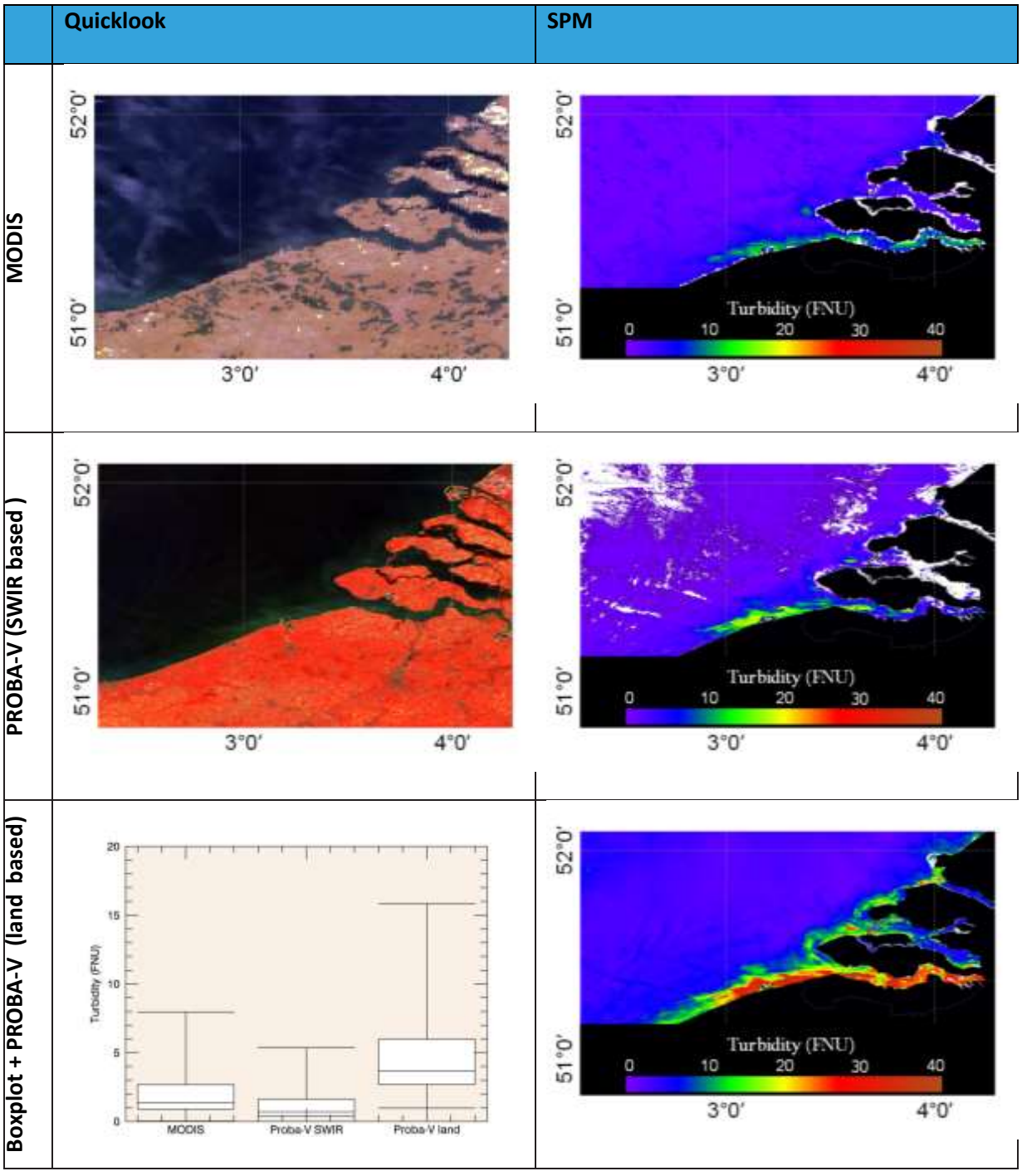

Figure 12: Quicklooks and turbidity maps generated for MODIS and PROBA-V, acquired on 03/04/2016. The latter using the iCOR-SWIR based and iCOR-land based method. The boxplots for the different results are plotted without outliers. Boxes represent the range between the 25th and 75th percentrile, while the whiskers represent the 5th and 95th percentile.

CHAPTER 4 A/C VALIDATION ADDITIONAL GLOBAL SITES

4.1. INTRODUCTION

In this section, the results of the A/C methods are shown for global test sites. The global AERONET-OC sites included are (i) Venise (Italy), (ii) Long Island Sound Coastal Observatory (LISCO) (New York, USA) and (iii) Martha's Vineyard Coastal Observatory (MVCO) (Massachusetts, USA).

The Venise AERONET-OC station is located at 45.31 °N, 12.50°E and altitude of 10 m, around 13 km from the shore. The global test validation site at LISCO is on western Long Island Sound 3.2 km offshore at New York, USA with coordinates 40.95° N, 73.34° W. The MVCO global validation test site (41.33°N; 70.57°W) is located 5 km offshore on the Air-Sea Interaction Tower, near Rhode island, USA with platform at 10 meter height. The locations of these stations are shown in Figure 13.

Figure 13: Location of the LISCO, MVCO Venise AERONET-OC stations.

For the Venise site, PROBA-V data from 2014 till 2016 have been processed both with land and SWIR-baseds A/C method. For the MVCO and LISCO only PROBA-V data from 2014 are processed.

No match-up analysis of the water leaving reflectance is performed, as no information was available to derive region specific spectral shift corrections, necessary to link the small spectral bands of AERONET-OC with the broad spectral bands of PROBA-V (see section 2.3.1).

4.2. AOT VALIDATION

Figure 14 gives the scatter plots of AERONET AOT versus PROBA-V retrieved AOT (550nm) values for respectively the land-based and the SWIR based A/C approach for the stations Venice, LISCO and MVCO.

There are less match-ups for the land-based compared to the SWIR-based for the Venice site. This is caused by cloud contamination over land: the iCOR land approach requires at least 50% of the 30 km x 30 km macro-pixel to be cloud-free for the AOT retrieval. As the PROBA-V subsets for the

Venice site were relatively small (i.e. 100 km x 100 km) there were several images for which no macro-pixels could be found with a cloud-percentage less than 50 %. For these images no AOT was retrieved. In the SWIR-based AC approach the AOT retrieval is pixel based. If according to the cloud mask (as provided in the status map of PROBA-V) the water-pixel is cloud free an AOT is retrieved in the SWIR-based approach.

The total amount of match-ups for the MVCO AERONET stations is very small (3 in total), as only a limited number of in-situ measurements fell within the 30 min restriction for match-up analysis. In iCOR SWIR based no results remained as these pixels were triggered by sun-glint.

We can observe in Figure 14 a lot of outliers in the SWIR-based results. Outliers (a) till (d) are linked to clouds and contrails at the AERONET-OC stations as illustrated in Figure 10. These clouds were not marked/detected as cloud in the status map provided with the PROBA-V data. Outlier (e) is caused by white caps/waves. Despite the outliers, similar regression coefficients were obtained using iCOR-SWIR for these global validation stations compared to the AOT validation of the North Sea: there is an offset of 0.14 and a slope of 1.02. iCOR land performs for these sites better than for the North Sea. Especially LISCO performs very well. The explanation can be found in the absolute distance from land: the further away from land, the more uncertainty and error propagation included in the extrapolation. The 26 km of shore for Thornton is most likely too far for the iCOR-land based retrieval to be valid.

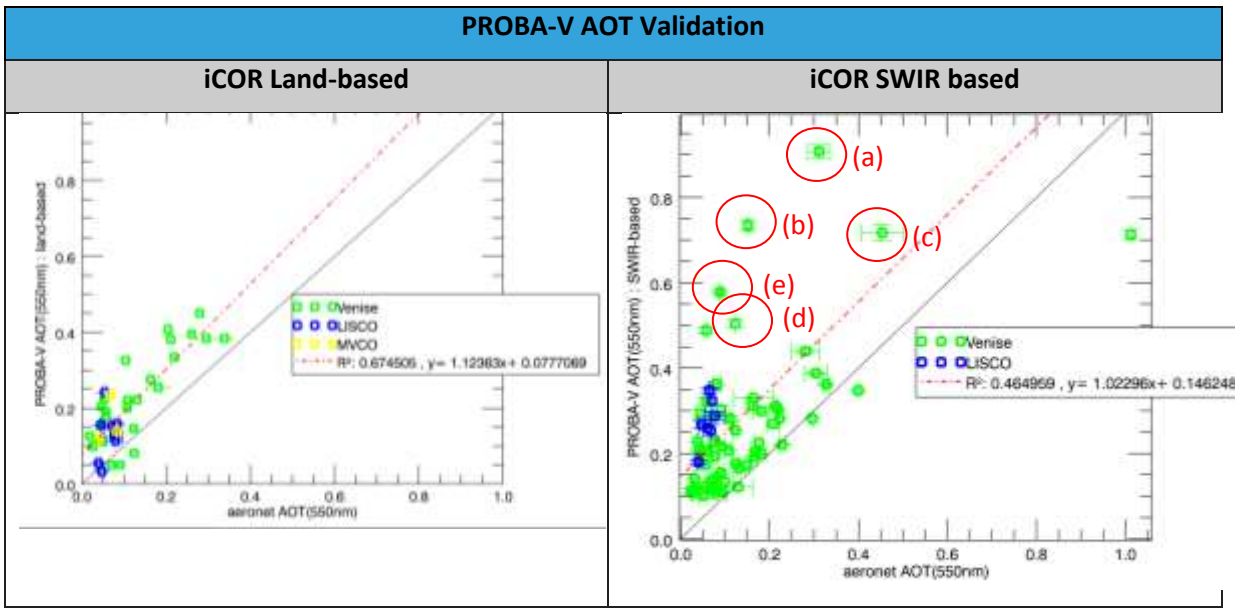

Figure 14 Scatter plots of AERONET AOT versus PROBA-V retrieved AOT (550nm) values for Venise, LISCO and MVCO sites. The solid black line is the 1:1 line, dotted RED line is the regression line.

(a)

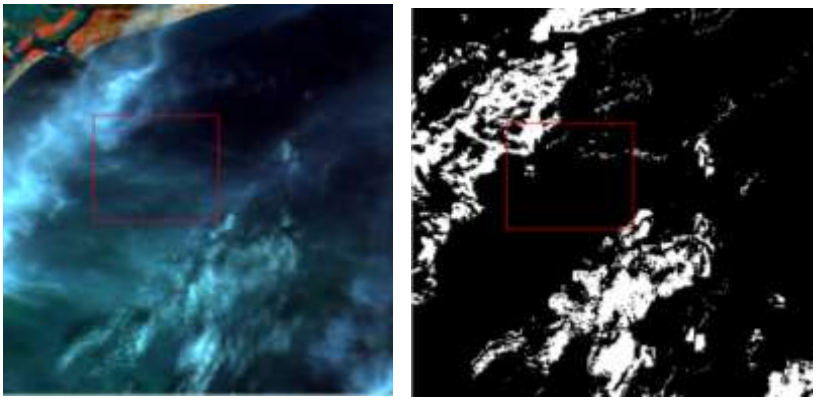

(b)

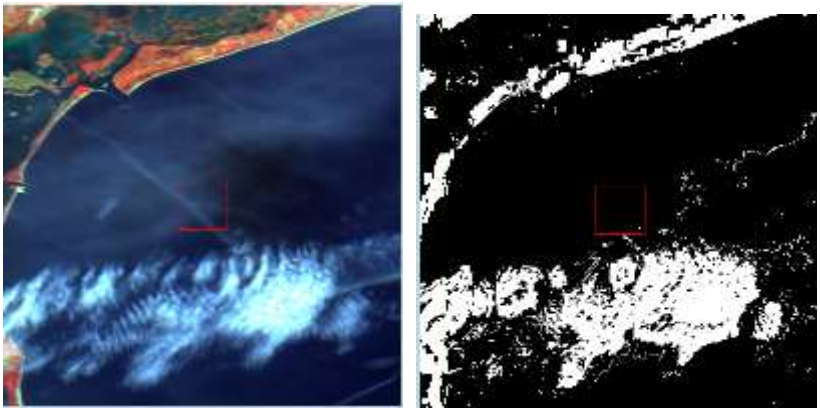

(c)

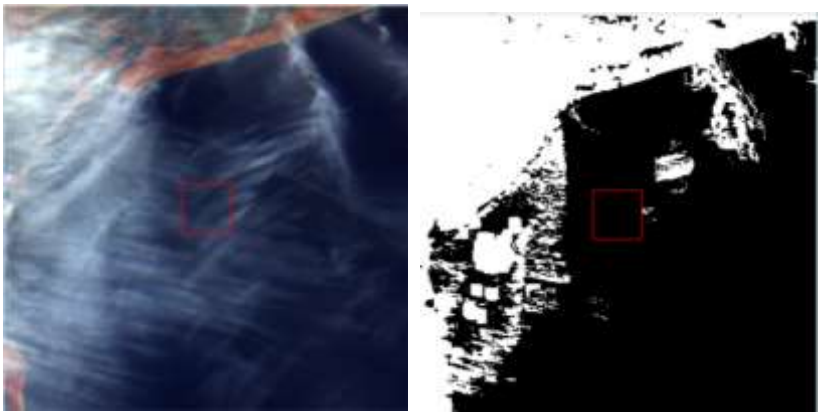

(d)

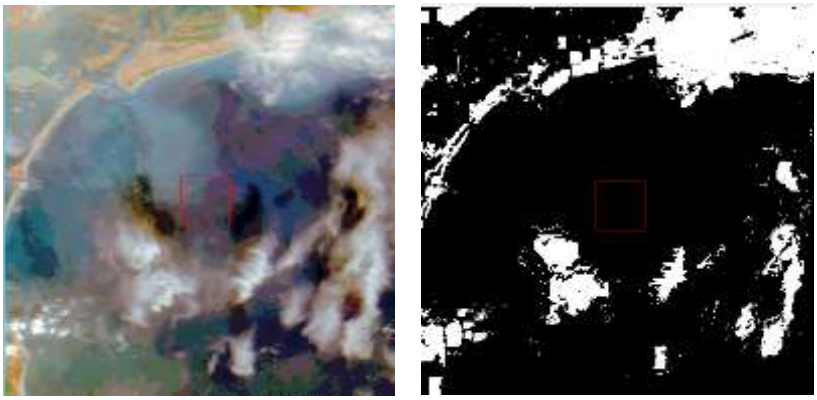

(e)

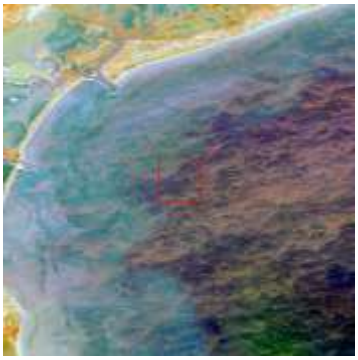

Figure 15 Visual inspection of outliers in Venice SWIR based AOT retrieval. Left : RGB image centered at AERONET-OC station; Right : Cloud mask (extracted from status map)

CHAPTER 5 CONCLUSIONS

PROBA-V data was processed, using two adaptations of iCOR: a land-based AOT retrieval method (iCOR-land) and the SWIR dark pixel approach (iCOR-SWIR). Different PROBA-V products were validated: (i) AOT values were compared with AERONET stations located near the North-Sea (Zeebrugge-MOW1 and Thornton C_power), Venice (Italy) and LISCO and MVCO (north-east USA), (ii) water leaving reflectance data was compared with the AERONET-OC stations in the North Sea and (iii) turbidity maps were validated against continuous in-situ instruments (e.g. CEFAS Smartbuoys) and MODIS products.

The AOT validation showed that iCOR-land performs relatively well in regions near the shoreline at global level. However, the further away from this shoreline, the more uncertain the results yielding low R^2 values, as was the case for the Thornton C_power station (26 km from shore). The iCOR-SWIR approach on the other hand seems to be consistent at first sight for the different test location considered, with an offset of 0.14 and a slope gradient of 1.02.

In order to fully validate the water leaving reflectance, spectral shift correction factors were applied to the narrow bands of the AERONET-OC data to make them comparable with the broad bands of PROBA-V. These spectral shift correction factors are region specific. As such, only results were derived for the North Sea, thanks to the availability of the extended CoastColour dataset. In this case the SWIR-based method showed the best results, with a maximum offset of 0.005 (band 668 nm), a slope of 0.91 (491 nm) and 1.02 (668 nm) and an R^2 higher or equal than 0.78. Only the VNIR band 870 nm showed in general a weak performance, but can be linked to the absence of spectral shift correction factor for this band. iCOR-land performs for all bands less accurate.

As a consequence, the turbidity values shows the best performance in the North Sea (R^2 of 0.73) using the iCOR-SWIR method, when validating with continuous in-situ instruments of CEFAS Smartbuoys. A comparison between PROBA-V and MODIS show that similar turbidity levels and patterns were found and the advantage of the higher spatial resolution of PROBA-V becomes visible in the Scheldt estuary.

In short, although PROBA-V was not intended to be used to derive water quality parameters, the radiometric performance is sufficient to derive information on the turbidity from the RED band in in moderate to high turbid waters. The iCOR-SWIR based method showed the best results, but closer to land a shift to iCOR-land might be favorable.

LITERATURE

Dogliotti, A., Ruddick, K., Nechad, B., Doxaran, D., Knaeps, E.,"A single algorithm to retrieve turbidity from remotely-sensed data in all coastal and estuarine waters", *Remote Sens. Environ.*, vol. 156, pages 157–168, 2015.

Mills, D. K., Laane, R.W. P.M., Rees, J. M., Loeff, M. R. V. D., Suylen, J. M., Pearce, D. J., et al.(2003). Smartbuoy: Amarine environmental monitoring buoy with a difference. In H. Dahlin, N. C. Flemming, K. Nittis, & S. E. Peterson (Eds.), *Building the European capacity in operational oceanography, proc. Third International Conference*

Nechad, B., Ruddick, K. and G. Neukermans, "Calibration and validation of a generic multisensor algorithm for mapping of turbidity in coastal waters", in Proceedings SPIE Vol. 7473, 74730H., 2009.

Roesler, C., and E. Boss. In situ measurement of the inherent optical properties (IOPs) and potential for harmful algal bloom detection and coastal ecosystem observations, p. 153–206. In M. Babin, C. Roesler, and J. Cullen [eds.], Realtime coastal observing systems for marine ecosystem dynamics and harmful algal blooms: Theory, instrumentation and modelling. UNESCO, 2008.